Colloids and Surfaces B: Biointerfaces 148 (2016) 278–286

Contents lists available at ScienceDirect

Colloids and Surfaces B: Biointerfaces

journal homepage: www.elsevier.com/locate/colsurfb

Orientation and biorecognition of immunoglobulin adsorbed on spin-cast poly(3-alkylthiophenes): Impact of polymer film crystallinity

Kamil Awsiuk[a,*], Andrzej Budkowski[a], Panagiota Petrou[b], Mateusz M. Marzec[c], Monika Biernat[a], Teresa Jaworska-Gołąb[a], Jakub Rysz[a]

[a] M. Smoluchowski Institute of Physics, Jagiellonian University, Łojasiewicza 11, 30-348 Kraków, Poland
[b] Institute of Nuclear & Radiological Sciences & Technology, Energy & Safety, NCSR Demokritos, 15310 Agia Paraskevi, Greece
[c] Academic Centre for Materials and Nanotechnology, AGH University of Science and Technology, Al. Mickiewicza 30, 30-059 Kraków, Poland

ARTICLE INFO

Article history:
Received 31 March 2016
Received in revised form 19 July 2016
Accepted 18 August 2016
Available online 20 August 2016

Keywords:
polythiophene
antibody orientation
time-of-flight secondary ion mass spectrometry
principal component analysis
X-ray photoelectron spectroscopy
atomic force microscopy

ABSTRACT

Many of bioelectronic and biosensor applications are based on poly(3-alkylthiophenes), conducting and solution-processable polymers. The most facile approach for the fabrication of such devices relies on biofunctionalization of P3AT surfaces with antibodies through adsorption. The success of this approach depends critically on antibody orientation that affects its biorecognition. As demonstrated here both these features are controlled by the surface structure of spin-cast P3ATs. In particular, a multi-technique and multivariate study that involved Atomic Force Microscopy, Grazing Incidence X-ray Diffraction, Angle-Resolved X-ray Photoelectron Spectroscopy, Enzyme-Linked ImmunoSorbent Assay, and Time-of-Flight Secondary Ion Mass Spectrometry combined with Principal Component Analysis is conducted in order to deduce the crystalline texture of three P3AT polymers as well as its effect on orientation of adsorbed rabbit immunoglobulin (IgG) molecules. An edge-on crystalline texture is concluded for regioregular poly(3-butylthiophene) (RP3BT) and poly(3-hexylthiophene) (RP3HT), while amorphous morphology is inferred for poly(3-butylthiophene) (P3BT). In addition, end-on and head-on orientations similar for all P3ATs were concluded, based on the amount of adsorbed rabbit IgG molecules. Examination of amino acids characteristic for $F(ab')_2$ and Fc fragments, and dominant in the external regions of adsorbed immunoglobulin molecules, points to end-on IgG alignment on RP3BT and RP3HT, but not on P3BT. Moreover, the binding of an anti-rabbit IgG antibody on the absorbed rabbit IgG is higher (up to 71%) when the biorecognition reactions are performed on regioregular rather than regiorandom P3AT surfaces. In particular, the highest biorecognition efficiency and IgG orientational order is observed for the RP3BT surfaces with the more developed crystallinity.

1. Introduction

Poly(3-alkylthiophenes) (P3ATs), known for their high charge mobility [1] and good solubility [2], form an archetypical class of conducting polymers [3] with increased potential for implementation in biomedical applications [4–8]. Easy solution processing of P3ATs [9], compatible with additive fabrication and flexible substrates enable the creation of various structures, that can be then applied for the fabrication of biosensors [4,7], printable bioelectronic devices [8] or scaffolds for tissue engineering and regeneration [3] since P3AT-based materials have been classified as biocompatible [10,11]. In addition, the electronic properties of P3AT polymers are expected to facilitate the transduction of molecular recognition events to biosensor signal [4,7], and enable electrical control of polymer and its interface [5,12]. Thus, they can find also application in implantable electrodes, controlled molecular release systems or bioseparation devices [3,13,14].

The conducting properties of the P3AT depend strongly on their microstructure [1]. P3AT macromolecules are made of a conjugated backbone of thiophene rings and solubility-providing alkyl side chains attached to the backbone in a pattern specified by head-to-tail (HT) couplings. HT regioregularity induces a crystalline order [15] that dramatically improves conductivity [15]. Solution-deposited films of regiorandom P3ATs are amorphous, but their

* Corresponding author.
E-mail address: kamil.awsiuk@uj.edu.pl (K. Awsiuk).

http://dx.doi.org/10.1016/j.colsurfb.2016.08.028
0927-7765/

regioregular counterparts are semi-crystalline with self-oriented crystallites [1]. In particular, the formation of edge-on textured crystallites, with separated layers of conjugated backbones and insulating alkyl groups forming the lamellae parallel to film substrate, results in significant enhancement of charge mobility.

The majority of the reported bioelectronic and biosensor applications of P3AT polymers rely on their functionalization with antibodies [6–8,13,14]. The attachment of the antibody molecules onto the P3AT films for biosensing applications is usually performed through covalent binding, which, however, has a negative impact on their electrical performance [6,8]. This has been ascribed to disturbance of thiophene rings arrangement by introduced functional groups linked to bulky bioreceptor proteins [6,8]. In contrast, direct physical adsorption of antibody onto P3AT films is considered as the functionalization method of choice [6,7], since it can be applied for the facile mass fabrication of biosensors based on organic thin-film transistors [7].

Nevertheless, to be able to effectively exploit the immobilized antibodies properties their antigen binding capacity should be preserved to a great extent upon immobilization onto transducer surface [16]. This is not an easy task since adsorption onto a surface induces changes in protein conformation [17,18] and leads to different antibody orientation [16,19–25] that could modify both reactivity and accessibility of the antigen-recognition sites. In our recent work [18], we have determined the impact of surface structure of RP3HT and P3BT on the adsorption and conformation of bovine serum albumin (BSA), a protein widely used to block biosensor surfaces against non-specific binding or to indirectly immobilize small molecular weight analytes in the form of conjugates. This study, concluded a higher degree of BSA denaturation on the RP3HT surfaces as compared to P3BT ones, as it was evidenced by determination of exposed hydrophobic residues [18].

The effects of antibody orientation on its bioactivity have been demonstrated for various substrates modifications and immobilization methods [6,16,20,22]. Nevertheless, such a study, at least to our knowledge, has not been performed for conducting polymers. Here, we examine how the surface structure, amorphous for P3BT and semi-crystalline for RP3BT and RP3HT, affects the *orientation* of a model antibody – rabbit immunoglobulin (IgG), upon its adsorption onto the polymer surface, as well as the immobilized IgG *biorecognition* by an anti-rabbit IgG antibody. To study these effects, we use as a tool constitutional isomerism in a way analogous to stereoisomerism applied to analyze structure-recognizing antibodies [26]. In particular, sequence isomers with identical formula but different bonding, P3BT and RP3BT, reveal a direct impact on modified IgG orientation and biorecognition due to the changed crystalline order of surface structure, resolved from the variations due to alkyl chain length using RP3BT and RP3HT.

The results section of this paper is organized as follows. First, the surface structure of P3ATs films with dissimilar crystalline order is discussed. Second, the amount of immunoglobulins adsorbed on P3AT surfaces is determined enabling selection of plausible molecular alignments. Then, the differences in IgG orientation on the various P3ATs substrates are discussed. Finally, the effect of substrate-induced orientation of adsorbed IgG molecules to their recognition by an anti-IgG antibody is examined.

2. Materials and methods

2.1. Materials

The polymers used in this work were poly(3-alkylthiophene)s (P3ATs) purchased from Sigma-Aldrich Chemical Co. (St. Louis, MO, USA): Poly(3-butylthiophene) (P3BT) was reported by the supplier to have a 1:1 ratio of head-to-head: head-to-tail linkages; regioregular poly(3-hexylthiophene) (RP3HT) and poly(3-butylthiophene) (RP3BT) were specified by head-to-tail regioregularity of >90.0% and 80–90%, respectively. Silicon wafers with native oxidized silicon layers (SiO_x) were obtained from Si-mat (Germany). Rabbit gamma globulins (IgG), HRP-conjugated polyclonal anti-rabbit IgG antibody, raised in goat against the whole IgG molecule (anti-IgG-HRP), and 2,2′-azinobis(3-ethylbenz-thiazoline sulfonic acid) diammonium salt (ABTS) were purchased by Sigma-Aldrich Chemical Co. (St. Louis, MO, USA). Bovine serum albumin (BSA; Cohn Fraction V) was obtained from ACROS Organics (Thermo Fisher Scientific; Geel, Belgium).

2.2. Sample preparation

Polymer films were spin-cast from analytical grade chlorobenzene (coating speed $\omega = 2.2$ krpm, solution concentration $C_P = 15$ mg/mL) and post-apply baked for 1 h at 60 °C prior to rabbit IgG adsorption. The spin-casting conditions (C_P,ω) determine the thickness h of polymer film [27], $h = A_h C_P/\omega^{1/2}$; this principle applies also to P3AT films [9]. The coefficient A_h relating film thickness with coating conditions was determined to be ~2.7, 3.9 and 3.3 nm krpm$^{1/2}$.mL/mg for P3BT, RP3BT and RP3HT, respectively. The surface wettability of polymer films was expressed by the water contact angle value, which was determined using the sessile drop technique (Kruss EasyDrop DSA15 instrument). Contact angle values equal to 91.9(1.7)°, 99.0(1.5)° and 103.2(6)° were found for P3BT, RP3BT and RP3HT, respectively.

Rabbit IgG was adsorbed to the surface of thin P3AT films through incubation for 1 h at RT from solutions with concentration C_{IgG} ranging from 5 μg/mL to 300 μg/mL prepared in 50 mM phosphate buffer, pH 7.4, followed by washing with buffer and distilled water, and drying under N_2 flow.

To evaluate biorecognition of adsorbed rabbit IgG from an anti-rabbit IgG antibody, after IgG adsorption from a solution with concentration of $C_{IgG} = 100$ μg/mL the surfaces were washed with 50 mM phosphate buffer, pH 7.4, and blocked via immersion in a 10 mg/mL BSA solution in 50 mM phosphate buffer, pH 7.4 (blocking buffer), for 1 h at RT. They then were washed with the 50 mM phosphate buffer, pH 7.4, and distilled water. After that, the samples were incubated with a 10 μg/mL solution HRP-conjugated anti-rabbit IgG antibody in blocking buffer for 1 h. The procedure was completed by washing with buffer and distilled water and drying under N_2 flow.

2.3. AFM surface examination

An Agilent 5500 atomic force microscope (AFM)[18,28,29] working in non-contact mode was used to examine the P3ATs surfaces in air prior to and after each step of proteins immobilization. AFM cantilevers (PPP-FMR, Nanosensors) with force constant of ~2 N/m, resonant frequency of ~75 kHz, and AFM tips with standard beam shape and small radius (<7 nm) were used. AFM micrographs were analyzed with the PicoImage software.

2.4. XPS surface characterization

Angle-resolved X-ray photoelectron spectroscopy (ARXPS) [18,28,29] spectra were recorded on a PHI 5000 VersaProbe II (ULVAC-PHI, Chigasaki) system using a micro-focused (100 μm, 25 W) Al Kα X-ray beam for three different values of photoelectron take-off angle Θ (10°, 30° and 45°), defined as the angle between the normal to the surface and the axis of the XPS analyzer lens. A dual-beam charge neutralizer was used to compensate the charge-up effect. High-resolution spectra were collected with analyzer pass energy of 46.95 eV. The operating pressure was less than 5×10^{-7} Pa. All XPS peaks were referenced to the neutral (C—C)

carbon C1 s peak, at a binding energy of 284.8 eV. Spectral backgrounds were subtracted using the Shirley method. All samples were measured in three non-overlapping spots.

2.5. ToF-SIMS surface examination

The P3ATs surfaces were analyzed prior to and after protein immobilization using time-of-flight secondary ion mass spectroscopy (ToF-SIMS) [18] (with a sampling depth of 1–1.5 nm). The TOF.SIMS 5 (ION-TOF GmbH) instrument was equipped with 30 keV bismuth liquid metal ion gun. Bi_3 clusters were used as the primary ions. The dose density deposited on the surface was identical for all samples and lower than 10^{12} ions/cm^2 (static mode conditions). Positive and negative ion static ToF-SIMS mass spectra were acquired from six different non-overlapping spots (200 μm × 200 μm) of 27 samples. The mass resolution $m/\Delta m > 5800$ at $C_4H_5^+$ ($m/z = 53$) and C_6^- ($m/z = 60$) peak for positive and negative spectra, respectively, was maintained.

2.6. Multivariate ToF-SIMS analysis with PCA

Principal component analysis (PCA) [18] was applied to two different sets of ToF-SIMS signals. This multivariate analysis technique was performed in order to examine: a) the exposure of alkyl side-chains on the surface of P3ATs thin films, and b) the orientation of adsorbed IgG molecules. For the first analysis the negative ion fragments corresponding to the alkyl side-chains and polythiophene backbones were selected. In turn, IgG orientation was assessed based on the positive ion peak list compiled from ToF-SIMS signals characteristic for amino acids [21,30]. The different sets of ToF-SIMS peaks selected for PCA in each case are specified in the corresponding figures. Prior to PCA, the intensities of the selected peaks from each spectrum were normalized to the sum of their intensities and then mean-centered. PCA was performed using PLS Toolbox (Eigenvector Research, Manson, WA) for MAT-LAB (MathWorks, Inc., Natick, MA).

2.7. ELISA assay

The recognition of adsorbed rabbit IgG by an anti-rabbit IgG antibody was evaluated through an enzyme-linked immunosorbent assay (ELISA) [31]. For this purpose, the spin-casted and post-apply baked P3ATs film surfaces were first incubated with a 100 μg/mL IgG solution in 50 mM phosphate buffer, pH 7.4, for 1 h at RT. They were then washed with the same buffer and blocked using the solution mentioned in Section 2.2 for three different time periods (15, 30, and 60 min). After washing with phosphate buffer, distilled water and drying under a stream of N_2, the samples were incubated with a 10 μg/mL solution of HRP-conjugated anti-rabbit IgG antibody in blocking buffer, for 1 h. Finally, after washing with phosphate buffer, the samples were transferred to plastic tubes containing 1 mL of enzyme substrate solution (0.03% H_2O_2, 1.9 mM ABTS in 0.1 M citrate–phosphate buffer, pH 4.5) and the solutions were stirred at RT. After 15 min, 100 μL aliquots from the solution in each tube were transferred to microtitration plates and the absorbance at 405 nm was measured by using the Multiscan RC microtitration plate reader (Labsystems, Finland). Non-specific binding was determined by using P3ATs film surfaces incubated in blocking buffer for 1 h and then in the HRP-conjugated anti-rabbit IgG antibody solution. Absorbance value was normalized to the sample surface. Samples were analyzed in duplicates, and absorbance was measured twice for each sample.

2.8. GIXD measurements

Out-of-plane X-ray diffraction measurements were performed on a PANAlytical Empyrean diffractometer (CuKα-radiation, fixed slits in the incident beam, a 0.18° parallel plate collimator and a PIXcel^{3D} detector in the diffracted beam). The grazing incidence X-ray diffraction (GIXD) [32] measurements were carried out for 2Θ between 3° and 15° (2Θ scan rate of 0.003°/min) at the angle of incidence ω = 0.3°. Each X-ray diffraction pattern is the sum of five consecutive measurements.

3. Results and discussion

3.1. Surface structure of P3AT films with different crystalline order

Constitutional isomers, a regiorandom P3BT and two regioregular P3ATs with different chain length, namely RP3BT and RP3HT, were used to spin-cast polymer films from chlorobenzene, a good solvent for all these polymers. The cast P3AT films were post-apply baked for 1 h at 60 °C, to minimize any solvent effect on protein adsorption [33]. All the results presented in this work refer to P3AT films prepared as described above.

3.1.1. Crystalline order of P3AT films determined from AFM, GIXD and PCA of ToF-SIMS data

The AFM micrographs acquired by AFM (Fig. 1) indicate a distinct crystalline order for regioregular and regiorandom P3ATs. In particular, a semi-crystalline morphology with randomly dispersed rod-like crystallites is revealed by the topographic AFM images for RP3BT (Fig. 1c). Fibrillar nanocrystals are evidenced by phase AFM images on RP3BT and also RP3HT surfaces (Fig. 1d,f), with phase contrast originating from the difference in the mechanical properties of crystalline and amorphous regions. Similar structures have been reported previously [1,18]. The fibrillar morphology is more pronounced for RP3BT than RP3HT suggesting higher crystallinity. This is also reflected on the surface roughness with root-mean-square average of height values, RMS, equal to 2.21(12) nm and 0.99(8) nm for RP3BT and RP3HT, respectively. In contrast, the featureless morphology of P3BT films in phase AFM micrographs, with the lower RMS value of 0.23(1) nm determined from topographic AFM images, indicates an amorphous surface structure (see Figs. 1a,b). The smooth surfaces of P3BT films are secured by the casting solvent, chlorobenzene, which has a very low vapor pressure ($P_{vp} = 1.2$ kPa), in contrast to substantial roughness of spin-cast films obtained when rapidly evaporating solvents are employed ($P_{vp} > 10$ kPa) [34]. The semi-crystalline surface structures of regioregular P3AT films depend on the particular conditions of solution deposition, such as the P3AT molecular weight, the solvent used, the casting method, the coating speed and the additional thermal treatment [1]. In addition, increase of edge-on oriented crystallites has been reported for decreasing alkyl side chain length (since the reduced solubility induces film formation with earlier initiated nucleation) [35]. Since edge-on oriented P3AT chains are related with nanofibrils [36], this accords with our observation of pronounced fibrillar morphology for RP3BT as compared to RP3HT films (Fig. 1c,d,f).

Polymer films were also examined with grazing incidence (out-of-plane) X-ray diffraction (GIXD). The GIXD data presented in Fig. 2a verify distinct crystalline order of regioregular and regiorandom P3ATs films: the diffraction patterns show a Bragg peak at ∼5.35° and ∼6.99° for RP3HT and RP3BT, respectively, whereas no peaks are observed for the amorphous films of regiorandom P3BT (Fig. 2c). The peak positions allow to calculate a lattice spacing equal to ∼1.26 nm and ∼1.65 nm for RP3BT and RP3HT, respectively. The

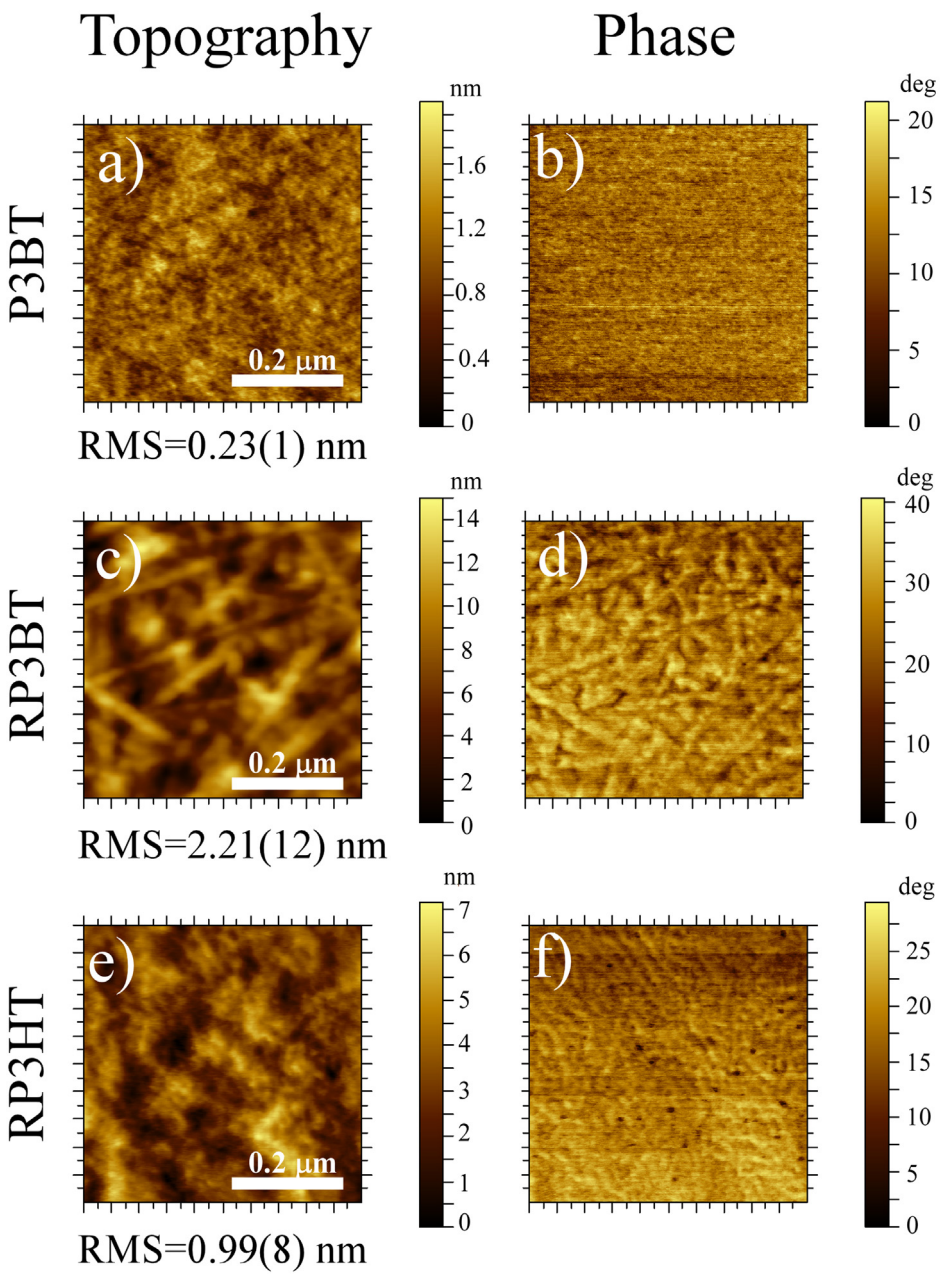

Fig. 1. Topographic (a,c,e) and phase (b,d,f) AFM images showing amorphous morphology of P3BT (a–b) and semi-crystalline microstructure of RP3BT (c–d) and RP3HT (e–f) films. Fibrillar morphology is more pronounced for RP3BT (c,d) than for RP3HT (f), suggesting higher crystallinity. RMS roughness values are the mean ± standard error of the mean determined from 6 images of two samples.

obtained values are in good agreement with the values reported for the (100) lattice planes of edge-on textured crystallites [32] (Fig. 2b). The longer the alkyl side chain, that separates the parallel to surface layers of polythiophene backbones, results in larger the interchain distance for RP3HT as compared to RP3BT. In turn, the integrated intensity of the Bragg peak is higher for RP3BT than for RP3HT, indicating higher crystallinity order for RP3BT.

The distinct film structures of regiorandom and regioregular poly(3-alkylthiophenes) imply different surface exposure of polythiophene backbones and alkyl side-chains [18]. As it has been demonstrated in our recent report [18], these two situations can be resolved with Principal Component Analysis of large ToF-SIMS data sets corresponding to negatively charged polymer fragment ions. A similar multivariate approach is applied also here, as described in details in the **Section S1** of Supplementary material. PCA reduces the dimensionality of ToF-SIMS data with the essential information retained by the first principal component PC1 (see **Fig. S1**), that explains most (86.08%) of the data variance. Positive PC1 values, corresponding to enhanced ion fragments of polythiophene backbones, are obtained for regiorandom P3BT, while negative PC1 scores, characteristic for alkyl side-chains, are determined for regioregular RP3BT and RP3HT films. In addition, the magnitude of negative scores on PC1 is somewhat smaller for RP3BT compared to RP3HT due to the shorter alkyl side-chains of this polymer. The effect of the edge-on textured crystallites is clearly demonstrated for the P3AT polymer with the same alkyl chain length (in contrast to Ref. [18]), when P3BT is compared with RP3BT.

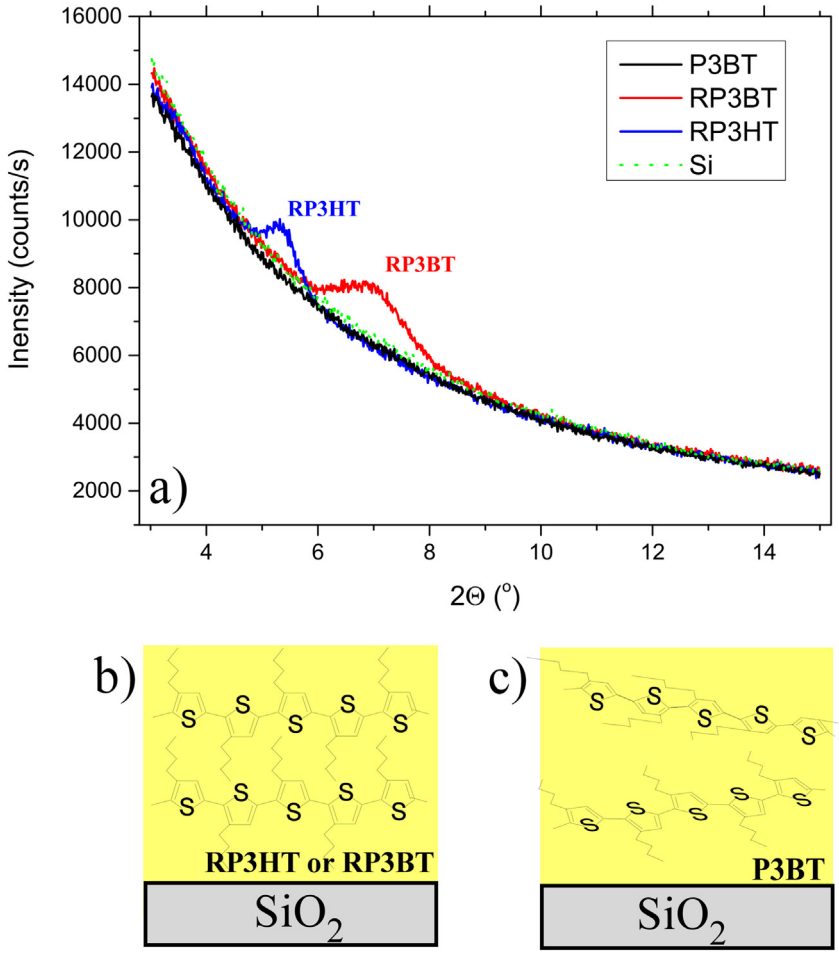

Fig. 2. Grazing incidence (out-of-plane) X-ray diffraction patterns (a) indicating the (100) diffraction peak for regioregular P3ATs originating from edge-on textured crystallites (b) (with alternating layers of alkyl side chains and polythiophene backbones oriented parallel to surface) [32]. In turn, amorphous films are suggested for P3BT (c). Note the larger intensity (synonymous to peak area) of the (100) peak for RP3BT in comparison to RP3HT, indicating higher crystallinity.

3.2. Adsorption of IgG on P3AT films.

3.2.1. IgG surface density determined from ARXPS

To evaluate the amount of IgG protein adsorbed on P3AT surfaces the angle-resolved XPS data were analyzed using a model introduced in previous publications [18,28,29] (see also **Section S2**). The determined surface densities of rabbit IgG adsorbed on the different P3AT surfaces are plotted in Fig. 3 as a function of the IgG concentration in the coating solution. The results are quite similar for all polymer surfaces. The immunoglobulin surface densities are identical for P3BT and RP3BT, with the RP3HT values being systematically lower but not statistically different from the values obtained for the two other surfaces (the mean values are within the ±error bars limits). The amount of IgG determined through adsorption experiments are in accord with those reported for RP3HT by other researchers (2.7 mg/m^2 for 50 μg/mL solution) [6]. In addition, the amount of antibody on the P3AT surfaces, with a value of 3.5 mg/m^2 for a maximum coverage, is at least two times higher when compared to amino-silanized SiO_2 surfaces [28].

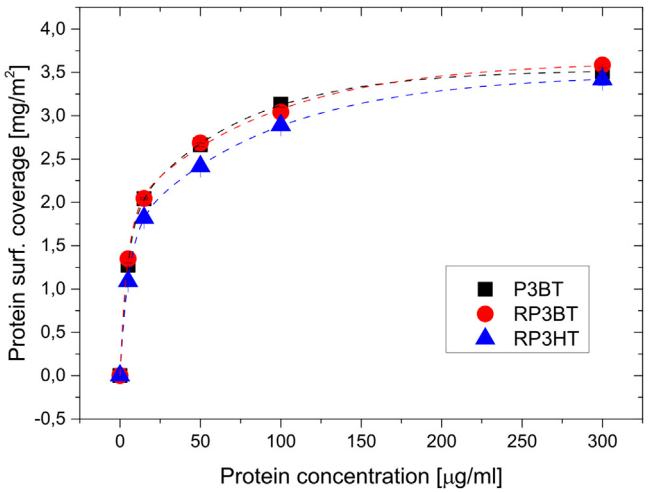

Fig. 3. The amount of rabbit IgG adsorbed on the surface of P3BT (squares), RP3BT (circles) and RP3HT (triangles) polymers determined with angle-resolved XPS as a function of IgG concentration in the coating solution. Dashed lines are a guide to eye.

3.2.2. Adsorption based preselection of immunoglobulins orientation

Immunoglobulins have a three-lobed structure, with two Fab fragments each one containing an antigen binding site and one crystallizable Fc fragment that is responsible for the activation of the cellular immune response. Due to its unique structure, immunoglobulins can adapt four distinct molecular orientations upon adsorption onto a surface leading to four specific values of *molecular* mass loading [22,23,37,38]: a flat-on (all three lobes attached to surface; 2.0 mg/m^2) [37], a side-on (Fc and one Fab at substrate with cross-sectional area of ~85 nm^2 ~2.9 mg/m^2) [37],

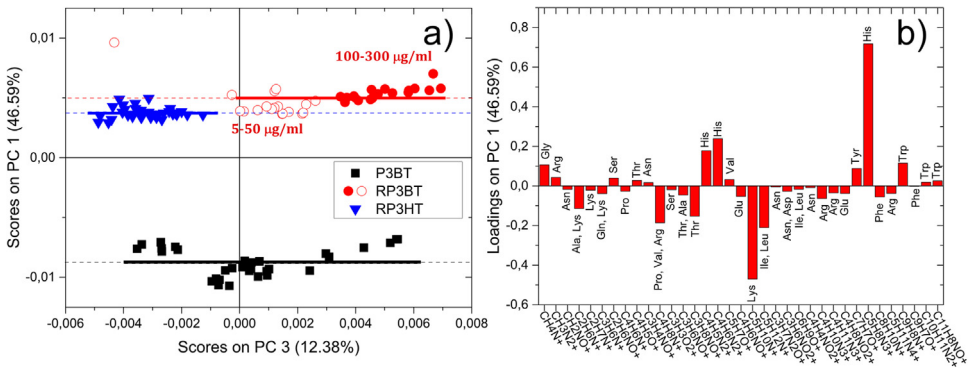

Fig. 4. (a) PCA scores plot of the positive ion ToF-SIMS spectra of rabbit IgG adsorbed on P3BT (squares), RP3BT (circles) and RP3HT (triangles) surfaces. The solid lines correspond for each polymer to the mean score on PC1 averaged over all the concentrations of IgG solution used for coating. For RP3BT, the data points corresponding to IgG concentration ranging from 5 to 50 μg/mL (open circles) and from 100 to 300 μg/mL (solid circles) are distinguished. (b) Corresponding loadings plot for the PC1. PCA distinguishes between ion fragments of amino acids dominant in the outer regions of IgG adsorbed to regioregular and regiorandom P3ATs that load the PC1 in the positive and negative direction, respectively.

an end-on (Fab-up, Fc attached to surface; 2.6–5.5 mg/m^2) [37] and finally a head-on (Fc-up, both Fabs attached to the substrate; 2.6–5.5 mg/m^2) [37]. In addition, the surface density values corresponding to the different orientations must be lower than *molecular* mass loadings, since adsorption cannot led to closely-packed IgG monolayers (coverage limit) [38]. Therefore, the relatively high (up to 3.5 mg/m^2) amount of IgG determined for all P3AT surfaces (Fig. 3), excludes both flat-on and side-on orientations to prevail in the adsorbed antibodies. Instead, the dominant molecular orientation of the immunoglobulins adsorbed onto P3AT surfaces might vary between end-on and head-on alignment both yielding identical surface densities. The above conclusion made for P3AT surfaces covered with an incomplete monolayer of IgG molecules is in agreement with our AFM results (see Section S3 in Supplementary material).

3.3. Orientation of immunoglobulins adsorbed on P3AT surfaces

3.3.1. Multivariate ToF-SIMS analysis of adsorbed IgG

To detect differences in amino acid composition on the outermost regions of immunoglobulins adsorbed to various P3AT films, multivariate PCA is applied to a set of 35 ToF-SIMS signals, specified in Fig. 4b, examined simultaneously for 108 recorded spectra. Generally, each secondary ion is a fragment of an individual amino acid but some ions correspond to a pair (Ala, Lys; Gln, Lys; Thr, Ala; Ile, Leu; Asn, Asp) or a triplet of amino acids (Pro, Val, Arg). The PCA results (Fig. 4a) reveal that the first principal component PC1 (explaining 46.59% of total variance) captures an interesting direction of the uncorrelated variation in the data set. In contrast, PC2 and PC3 are not informative (PC3 is used merely to separate the measurements with similar PC1 values). The PC1 scores plot (Fig. 4a) clearly distinguishes between amino acids dominant in the external regions of rabbit IgG immobilized on regioregular P3ATs, exhibiting positive PC1 values, and those adsorbed on regiorandom P3BT (marked with squares), having negative PC1 scores. In addition, two further distinctions between the data points presented in Fig. 4a can be deduced. Firstly, the magnitude of positive PC1 scores, averaged over the different samples (the solid lines marked in Fig. 4a), is larger for the IgG immobilized on the RP3BT (circles) rather than the RP3HT films (triangles). Secondly, the PC1 values obtained for the antibody adsorbed on the RP3BT substrate are somewhat larger when IgG solutions with concentration equal to or higher than 100 μg/mL are used for coating (solid circles). The positive and negative PC1 scores (Fig. 4a) are induced by positive and negative loadings on PC1 (Fig. 4b) and originate from different magnitude of various amino acid ion fragments. A detailed interpretation of these PC1 loadings is provided in the following section.

3.3.2. Immunoglobulin orientation from multivariate ToF-SIMS analysis

To interpret subtle differences in the outermost surface composition of immunoglobulin adsorbed on the different P3AT polymers based on amino acid ion fragments recorded with ToF-SIMS, we examine the PC1 loading plot (Fig. 4b) taking into account the different molecular orientations.

In particular, two orientations are selected based on the IgG adsorption results, the end-on and head-on alignment, which result in different exposure of the F(ab')$_2$ and Fc fragments onto the surface. To resolve the end-on from the head-on orientation, the percent ratio of each amino acid in the F(ab')$_2$ and the Fc fragments could be used [21,39]. However, as noted above some of the observed ToF-SIMS signals do not correspond to individual amino acids but pairs or even triplets of them (Fig. 4b). Therefore, we apply a more general parameter, referring to all the ToF-SIMS signals, but consistent with the F(ab')$_2$/Fc composition ratio [21]. This is the relative prevalence, RP, of amino acid ion fragments originating from the F(ab')$_2$ versus the Fc fragments, extended from that introduced by Wang et al.[21], and plotted in Fig. 5a against the loadings on PC1 (from Fig. 4b). The RP parameter is defined (as a principal component) by the results of PCA performed [21] for ToF-SIMS spectra of a model antibody molecule and its reference fragments, F(ab')$_2$ (negative RP values) and Fc (positive PR values). Fig. 5a compares the RP parameter values [21] with the PC1 loadings determined in this work for identical ion fragments (squares) and/or amino acids (circles). As it can be concluded (Fig. 5a) the outer regions of IgG adsorbed to regioregular P3AT (positive PC1 values) are dominated by the F(ab')$_2$ portion of the molecule (negative RP), while the exposed regions of IgG immobilized onto regiorandom P3BT (negative PC1 loadings) correspond both to the Fc and F(ab')$_2$ fragments. Therefore, a dominant end-on (Fig. 5b) and a mixed end-on/head-on (Fig. 5c) orientation is concluded for adsorption of IgG molecules on regioregular and regiorandom P3AT polymers, respectively. With this interpretation, we could reanalyze the data plotted in Fig. 4a for regioregular P3ATs to point out two additional distinctions. The PC1 scores, higher for IgG on RP3BT (circles) than RP3HT (triangles), must reflect to some extent the higher orientational order of the end-on molecular alignment on this polymer. The same is true for immunoglobulins adsorbed on RP3BT from solutions with high IgG concentration (solid circles).

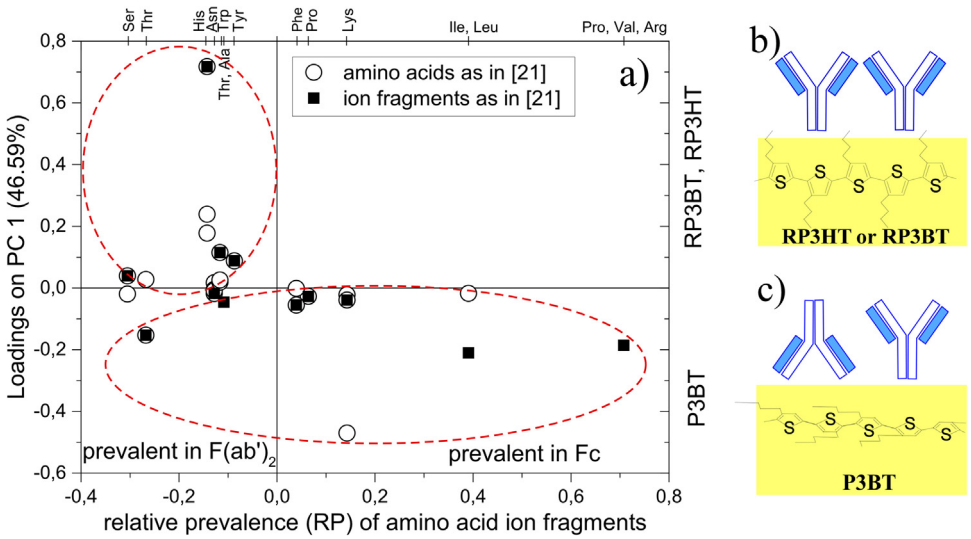

Fig. 5. (a)Loadings on PC1 (shown in Fig. 4b), corresponding to IgG adsorbed to regioregular (positive PC1 values) and regiorandom P3ATs (negative PC1 values) plotted as a function of relative prevalence, RP, of amino acid ion fragments originating from the $F(ab')_2$ versus the Fc fragment. The RP parameter is defined by the results of PCA performed [21] for ToF-SIMS spectra of a model antibody molecule and its fragments $F(ab')_2$ (negative RP values) and Fc (positive RP values). Marked are the ion fragments and/or amino acids identical to those of the Ref. [21]. Ellipses mark schematically the concluded exposure of antibody fragments: $F(ab')_2$ for RP3BT and RP3HT corresponding to a dominant end-on orientation (b), both Fc and $F(ab')_2$ for P3BT corresponding to a mixed head-on/end-on orientation (c).

3.3.3. Immunoglobulin orientation controlled by the substrate

Charge distribution within the IgG molecule can be induced even at pH values close to its isoelectric point (IEP), due to the fact that the Fc and $F(ab')_2$ fragments, have different IEP values and thus, are negatively and positively charged, respectively at these pH values [21,22,40]. Thus, the whole IgG molecule has a dipole momentum pointing from Fc to $F(ab')_2$ fragment. Alignment of the formed dipole with end-on (Fc down) and head-on ($F(ab')_2$ down) orientation, depends on the strength of electrostatic interactions with the substrate, as it has been reported for antibodies immobilized on self-assembled monolayers [21,22,40].

This antibody orientation model [21,22,40] could be extended tentatively to P3AT polymer surfaces. Polythiophenes are electroactive polymers known for strong electrostatic interactions with antibodies [13,14]. For instance, upon contact with antibody solution they can turn to positively charged conjugated backbones, counter-balanced by the antibodies acting as molecular dopant anions [14]. For the regioregular P3AT surfaces, the positively charged conjugated backbones form a well-ordered and densely packed chains in the edge-on oriented crystallites covered by insulating alkyl side-groups. Thus, the electrostatic interactions of the substrate with the IgG molecules are expected to favor the positioning of the negatively charged Fc fragment to be located closer to the surface, resulting in the 'end-on' orientation of the IgG molecule. In turn, the amorphous surfaces of regiorandom P3AT, with disordered polymer chains, are expected to result in less effective electrostatic field hence leading to a mixed end-on/head-on IgG orientation. This model explains also two additional features of the results presented in Fig. 4a. The effective field ordering IgG molecules would be enhanced for the surfaces with higher crystallinity as compared to less crystalline ones, hence leading to higher orientational order and PC1 scores for IgG adsorbed on RP3BT rather than RP3HT. In addition, the end-on orientation of IgG molecules is expected to be more pronounced when the IgG surface density on RP3BT substrates is increased, taking advantage of the inter-molecular interactions between $F(ab')_2$ fragments.

Apart from the described mechanism that governs IgG orientation on P3AT, another one induced by the surface nanostructuring and its effect on optimal protein density could be considered [41]. However, this model is not applicable here since, as it has been already mentioned, the surface density of adsorbed IgG is quite similar for all P3AT surfaces. In addition, the difference in RMS roughness between P3AT surfaces (<2 nm) is quite small, as compared to the values (~8 nm) reported to affect protein adsorption [42].

3.4. Biorecognition of immunoglobulins adsorbed on P3AT surfaces

It is of interest to compare and relate orientation of adsorbed immunoglobulins, determined with PCA of ToF-SIMS data, with biorecogntion experiment results [20]. For this purpose, the P3AT surfaces, after adsorption of rabbit immunoglobulin, were blocked with bovine serum albumin to prevent non-specific adsorption, and then probed with a secondary polyclonal anti-rabbit IgG antibody, raised in goat against the whole IgG molecule and conjugated with HRP, in order to quantify the recognition of adsorbed IgG.

The whole procedure is also monitored by AFM (**Fig. S2**) and multivariate ToF-SIMS (**Fig. S3**) after each functionalization/reaction step so as to record changes in surface nanostructure and chemistry after each individual step (see **Section S3**).

3.4.1. Biorecognition estimation using ELISA

The relative amount of anti-IgG antibody-HRP conjugate bound to the rabbit IgG-coated P3AT surfaces was determined through an enzyme-linked immunosorbent assay. The results obtained from the various P3AT polymers coated with rabbit IgG, blocked with BSA solution for 15, 30 and 60 min, and then reacted with the anti-rabbit IgG antibody are provided in Fig. 6a. As shown, independently of the blocking time, when the rabbit IgG is adsorbed on the regioregular P3AT surfaces, a 31–71% higher biorecognition from the HRP-conjugated secondary antibody is observed as compared to regiorandom P3AT surfaces, indicating a larger amount of rabbit IgG molecule epitopes exposed to the anti-rabbit IgG antibody. This accords with the conclusions from the multivariate ToF-SIMS analysis, since a more accessible IgG molecule is expected when the molecule is adsorbed adopting an end-on orientation ($F(ab')_2$ up) upon adsorption onto regioregular P3ATs rather than with a head-on alignment on, regiorandom P3ATs. These two orientations were

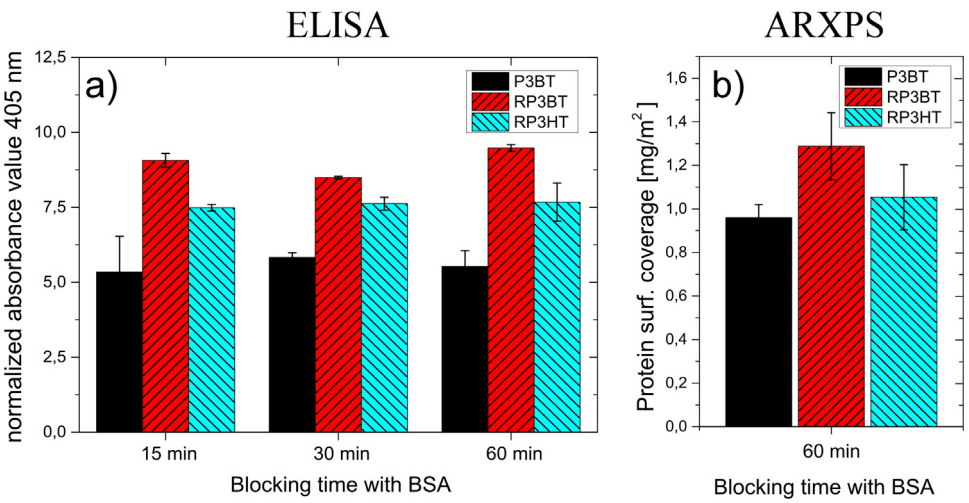

Fig. 6. Biorecognition of rabbit IgG adsorbed from a 100 μg/mL solution onto different polymer surfaces (P3BT, RP3BT, RP3HT) by an anti-rabbit IgG antibody conjugated to HRP. All surfaces have being blocked for 15, 30 or 60 min through incubation with a BSA solution. (a) The relative amount of anti-rabbit IgG antibody-HRP conjugate that has reacted with the adsorbed rabbit IgG as determined by ELISA (bars correspond to mean values ± standard deviation, n = 4). (b) The absolute amount of bound anti-rabbit IgG antibody-HRP conjugate evaluated with angle-resolved XPS.

confirmed, based on the amount of adsorbed rabbit immunoglobulin.

In addition, the ELISA results presented in Fig. 6 show that the biorecognition of the adsorbed IgG molecules is to some extent higher on the RP3BT rather than the RP3HT surfaces. This is in agreement with the enhanced orientational order of IgG, concluded for the RP3BT surfaces with higher crystallinity.

Based on previous data about the adsorption and denaturation of BSA molecules onto regioregular P3AT films [18], one should expect increased denaturation of rabbit IgG molecules and therefore, reduced accessibility of rabbit IgG epitopes by the secondary antibody. Nevertheless, the results presented in Fig. 6a indicate a rather minor effect on biorecogntion due to IgG denaturation by the edge-on crystalline texture of regioregular P3ATs.

3.4.2. Biorecognition estimation confirmed with ARXPS

The absolute amount of anti-rabbit IgG antibody-HRP conjugate bound to the P3AT surfaces that have been coated with rabbit IgG was determined indirectly from angle-resolved XPS (see **Section3.2**), as the difference between protein surface density prior to and after immunoreaction. The values determined for the different P3AT surfaces (Fig. 6b) confirm those obtained for the various substrates with the ELISA (cf. Fig. 6a).

4. Conclusion

Control and monitoring of biomolecular interactions at the surfaces of poly(3-alkylthiophenes) and their derivatives has led to numerous applications in the area of bioelectronics [3,5,14] and biosensors [6,7,8,43], that often rely on *spin-cast* polymer films biofunctionalized with *adsorption of* antibodies [6,7,8,43]. The performance of such devices depends to a great extent on the biological activity of the immobilized antibody that can be affected by surface induced changes in antibody orientation modifying the accessibility of its antigen-recognition sites [16,19–25]. Although several in depth studies have aimed at understanding and control the adsorbed antibody orientation and/or biorecognition as a function of surface modification on various substrates [16,19–23], such a study has not been performed for conducting polymer surfaces.

In the present study, both the orientation and biorecogntion of model antibody *adsorbed* on *spin-cast* films of different sequence isomers of poly(3-alkylthiophenes) with distinct surface structures have been examined. Regioregular P3ATs films are observed to form semi-crystalline surface structure with edge-on texture that promotes end-on immunoglobulin orientation leading to increased (up to 71%) biorecognition of adsorbed molecules. This finding in conjunction with the enhanced charge mobility of regioregular P3AT polymer films with edge-on textured semi-crystalline structure supports their implementation as substrates for bioelectronics and biosensing devices. On the other hand, the amorphous regiorandom P3AT films led to lower order of adsorbed immunoglobulins (with mixed end-on/head-on orientation) and reduced biorecognition efficiency by a secondary anti-IgG antibody.

Acknowledgments

This work was supported by the Polish National Science Center (NCN) under the Grant No. UMO-2011/03/N/ST5/04764, equipment purchased thanks to the financial support of the European Regional Development Fund (POIG.02.01.00-12-023/08) and the European Regional Development Found Operational Program Infrastructure and Environment (POIS 13.01.00-00-062/08).

Appendix A. Supplementary data

Supplementary data associated with this article can be found, in the online version, at http://dx.doi.org/10.1016/j.colsurfb.2016.08.028.

References

[1] A. Salleo, Mater. Today 10 (2007) 38–45.
[2] J. Jaczewska, A. Budkowski, A. Bernasik, I. Raptis, J. Raczkowska, D. Goustouridis, J. Rysz, M.J. Sanopoulou, Appl. Polym. Sci. 105 (2007) 67–79.
[3] M.J. Higgins, P.J. Molino, Z. Yue, G.G. Wallace, Chem. Mater. 24 (2012) 828–839.
[4] M. Magliulo, M.Y. Mulla, M. Singh, E. Macchia, A. Tiwari, L. Torsi, K.J. Manoli, Mater. Chem. C 3 (2015) 12347–12363.
[5] R.B. Pernites, C.M. Santos, M. Maldonado, R.R. Ponnapati, D.F. Rodrigues, R.C. Advincula, Chem. Mater. 24 (2012) 870–880.
[6] W.M. Albers, J.M. Pelto, C. Suspène, J.A. Määttä, A. Yassar, V.P. Hytönen, I.M. Vikholm-Lundin, K. Tappura, ACS Appl. Mater. Interfaces 4 (2012) 4067–4077.
[7] P. Lin, F. Yan, Adv. Mater. 24 (2012) 34–51.
[8] K. Manoli, M. Magliulo, M.Y. Mulla, M. Singh, L. Sabbatini, G. Palazzo, L. Torsi, Angew. Chemie Int. Ed. 54 (2015) 12562–12576.
[9] J. Jaczewska, A. Budkowski, A. Bernasik, I. Raptis, E. Moons, D. Goustouridis, J. Haberko, J. Rysz, Soft Matter 5 (2009) 234–241.

[10] A.S. Widge, M. Jeffries-El, X. Cui, C.F. Lagenaur, Y. Matsuoka, Biosens. Bioelectron. 22 (2007) 1723–1732.
[11] G. Scarpa, A.-L. Idzko, S. Götz, S. Thalhammer, Macromol. Biosci. 10 (2010) 378–383.
[12] X. Wang, T. Ederth, O. Inganäs, Langmuir 22 (2006) 9287–9294.
[13] G. Wallace, G. Spinks, Soft Matter 3 (2007) 665.
[14] G.G. Wallace, L.A. Kane-Maguire, P. Adv. Mater. 14 (2002) 953–960.
[15] T.A. Chen, X. Wu, R.D. Rieke, J. Am. Chem. Soc. 117 (1995) 233–244.
[16] N. Tajima, M. Takai, K. Ishihara, Anal. Chem. 83 (2011) 1969–1976.
[17] P. Roach, D. Farrar, C.C. Perry, J. Am. Chem. Soc. 127 (2005) 8168–8173.
[18] K. Awsiuk, A. Budkowski, M.M. Marzec, P. Petrou, J. Rysz, A. Bernasik, Langmuir 30 (2014) 13925–13933.
[19] X. Zhao, F. Pan, B. Cowsill, J.R. Lu, L. Garcia-Gancedo, A.J. Flewitt, G.M. Ashley, J. Luo, Langmuir 27 (2011) 7654–7662.
[20] V. Lebec, S. Boujday, C. Poleunis, C.-M.M. Pradier, A. Delcorte, J. Phys. Chem. C 118 (2014) 2085–2092.
[21] H. Wang, D.G. Castner, B.D. Ratner, S. Jiang, Langmuir 20 (2004) 1877–1887.
[22] S. Chen, L. Liu, J. Zhou, S. Jiang, Langmuir 19 (2003) 2859–2864.
[23] M.E. Wiseman, C.W. Frank, Langmuir 28 (2012) 1765–1774.
[24] A. Trilling, J. Beekwilder, H. Zuilhof, Analyst 138 (2013) 1619–1627.
[25] F. Liu, M. Dubey, H. Takahashi, D.G. Castner, D.W. Grainger, Anal. Chem. 82 (2010) 2947–2958.
[26] L. Addadi, N. Rubin, L. Scheffer, R. Ziblat, Acc. Chem. Res. 41 (2008) 254–264.
[27] P. Cyganik, A. Budkowski, U. Steiner, J. Rysz, A. Bernasik, S. Walheim, Z. Postawa, J. Raczkowska, U. Budkowski, J. Steiner, A. Rysz, S. Bernasik, Z. Walheim, J.R. Postawa, Europhys. Lett. 62 (2003) 855–861.
[28] K. Awsiuk, A. Bernasik, M. Kitsara, A. Budkowski, P. Petrou, S. Kakabakos, S. Prauzner-Bechcicki, J. Rysz, I. Raptis, Colloids Surf. B. Biointerfaces 90 (2012) 159–168.
[29] K. Awsiuk, A. Bernasik, M. Kitsara, A. Budkowski, J. Rysz, J. Haberko, P. Petrou, K. Beltsios, J. Raczkowska, Colloids Surf. B. Biointerfaces 80 (2010) 63–71.
[30] M.S. Wagner, D.G. Castner, Langmuir 17 (2001) 4649–4660.
[31] A.M. Douvas, P.S. Petrou, S.E. Kakabakos, K. Misiakos, P. Argitis, E. Sarantopoulou, Z. Kollia, A.C. Cefalas, Anal. Bioanal. Chem. 381 (2005) 1027–1032.
[32] T. Erb, U. Zhokhavets, G. Gobsch, S. Raleva, B. Stühn, P. Schilinsky, C. Waldauf, C.J. Brabec, Adv. Funct. Mater. 15 (2005) 1193–1196.
[33] J. Zemła, M. Lekka, J. Raczkowska, A. Bernasik, J. Rysz, A. Budkowski, Biomacromolecules 10 (2009) 2101–2109.
[34] K.E. Strawhecker, S.K. Kumar, J.F. Douglas, A. Karim, Macromolecules 34 (2001) 4669–4672.
[35] S. Thankaraj Salammal, S. Dai, U. Pietsch, S. Grigorian, N. Koenen, U. Scherf, N. Kayunkid, M. Brinkmann, Eur. Polym. J. 1 (2015) 199–212.
[36] H. Yang, S.W. Lefevre, C.Y. Ryu, Z. Bao, Appl. Phys. Lett. 90 (2007) 172116.
[37] J. Buijs, J.W.T.T. Lichtenbelt, W. Norde, J. Lyklema, Colloids Surf. B. Biointerfaces 5 (1995) 11–23.
[38] M. Dąbkowska, Z. Adamczyk, Colloids Surf. B. Biointerfaces 118 (2014) 57–64.
[39] E. Kosobrodova, R.T. Jones, A. Kondyurin, W. Chrzanowski, P.J. Pigram, D.R. McKenzie, M.M. Bilek, M. Acta Biomater. 19 (2015) 128–137.
[40] H. Chen, J. Huang, J. Lee, S. Hwang, K. Koh, Sensors Actuators B. Chem. 147 (2010) 548–553.
[41] E.E. Bedford, S. Boujday, C.-M. Pradier, F.X. Gu, RSC Adv. 5 (2015) 16461–16475.
[42] B. Müller, M. Riedel, R. Michel, S.M. De Paul, R. Hofer, D. Heger, D. Grützmacher, J. Vac. Sci. Technol. B Microelectron. Nanom. Struct. 19 (2001) 1715.
[43] M. Magliulo, D. De Tullio, I. Vikholm-Lundin, W.M. Albers, T. Munter, K. Manoli, G. Palazzo, L. Torsi, Anal. Bioanal. Chem. 408 (2016) 3943–3952.